Chinese Journal of Polymer Science Vol. 32, No. 10, (2014), 1276−1285

Chinese Journal of Polymer Science
© Chinese Chemical Society
Institute of Chemistry, CAS
Springer-Verlag Berlin Heidelberg 2014

Synergistic Effect of Carbon Nanotubes and Layered Double Hydroxides on the Mechanical Reinforcement of Nylon-6 Nanocomposites*

Tianxi Liu[a, b**], Hongdan Peng[b], Yue-E Miao[b], Weng Weei Tjiu[c], Lu Shen[c] and Chun Wei[a**]

[a] *Key Laboratory of New Processing Technology for Nonferrous Metals and Materials, Ministry of Education, College of Materials Science and Engineering, Guilin University of Technology, Guilin 541004, China*

[b] *State Key Laboratory of Molecular Engineering of Polymers, Department of Macromolecular Science, Fudan University, Shanghai 200433, China*

[c] *Institute of Materials Research and Engineering, A*STAR (Agency for Science, Technology and Research), 3 Research Link, Singapore 117602*

Abstract Synergistic effect in network formation of nylon-6 (PA6) nanocomposites containing one dimensional (1D) multi-walled carbon nanotubes (CNTs) and two dimensional (2D) layered double hydroxide (LDH) platelets on improving the mechanical properties has been studied. Mechanical tests show that, with incorporation of 1 wt% LDHs and 0.5 wt% CNTs, the tensile modulus, the yield strength as well as the hardness of the ternary composite are greatly improved by about 230%, 128% and 110% respectively, as compared with neat PA6. This is mainly attributed to the unique, strong interactions between the CNTs and the LDHs as well as the jammed network-like structure thus formed between the nanofillers, as confirmed by the morphological observations. As compared with the binary nanocomposites, a much enhanced solid-like behavior in the terminal region of the rheological curves can clearly be observed for the ternary system, which also indicates the formation of a percolating filler network.

Keywords: Nylon 6; Nanocomposites; Carbon nanotubes; Layered double hydroxide; Mechanical properties.

INTRODUCTION

In the large field of nanotechnology, polymer matrix based nanocomposites have become a prominent area of current research and development[1]. Owing to the nano-sized particles obtained by fine dispersion, these nanocomposites exhibit remarkable improvements in mechanical, thermal, optical and physico-chemical properties when compared with pure polymer or conventional (micro)composites as demonstrated by Kojima and coworkers for nylon-6 (PA6)/clay hybrids[2]. Previous studies on the layered inorganic materials have mainly been focused on the layered silicate nanocomposites, because of the relatively low layer charge density and the easy intercalation/exfoliation of montmorillonite-type layered silicate compounds[3−5].

Nevertheless, in the last decade, much attention has been turned to hydrotalcite-like layered double hydroxides (LDHs), the most well known anionic clays, as novel two-dimensional (2D) reinforcing nanofillers for polymers[6, 7]. LDHs consist of positively charged metal hydroxide sheets with anions (along with water) located between the layers to compensate the charge on the layers, which present the advantage of a large variety

* This work was financially supported by the National Natural Science Foundation of China (No. 51125011), Guangxi Small Highland Innovation Team of Talents in Colleges and Universities, Guangxi Funds for Specially-appointed Experts, and Guangxi Natural Science Foundation of China (No. 2014GXNSFAA118321).

** Corresponding authors: Tianxi Liu (刘天西), E-mail: txliu@fudan.edu.cn
Chun Wei (韦春), E-mail: 1986024@glut.edu.cn

Received April 22, 2014; Revised June 4, 2014; Accepted June 11, 2014
doi: 10.1007/s10118-014-1521-y

of compositions, a tunable charge density and allowing multiple interactions with polymers over natural clays[8, 9]. They are good candidates for inorganic constituents in polymer nanocomposites because of their excellent thermal/mechanical stability and unique tunnel structure. Besides, LDHs present a great number of hydroxide groups, making them attractive as fire-retardant additives in polymers[10]. On the other hand, carbon nanotubes (CNTs), as typical one-dimensional (1D) nanomaterials, are currently employed as ideal enhancement fillers in polymer matrix to produce nanocomposites with high mechanical strength and multifunctionality[11–14]. CNT reinforced PA6 composite is one of the most studied systems in the past years[15–20]. For example, Gao *et al*. reported the preparation of single-walled carbon nanotubes (SWNT)/PA6 composites by *in situ* polymerization of caprolactam in the presence of carboxylic acid[15] and amide functionalized SWNTs[16]. The resulting composites show good dispersion of SWNTs and significant improvements in Young's modulus and tensile strength due to the grafting of nylon chains on SWNTs. However, the potential of employing CNTs as reinforcing fillers is usually limited by the difficulties associated with the dispersion of entangled CNTs during processing, especially at high nanotube loadings and/or poor interfacial interaction with the matrix.

As the enhanced properties are usually "saturated" due to the filler aggregation, particularly at high filler contents[21], it is obviously difficult to further improve the mechanical properties of PA6 by using only CNTs or LDHs alone. Therefore, hybrid composites with different mixtures have lately attracted increasing attentions, such as CNTs with carbon black[22], few layer graphene with SWNTs and nano diamonds[23], and CNTs with graphitic nanoplatelets (GnP)[24]. Kumar *et al*.[24] reported that CNTs and GnP form a co-supporting hybrid network in which the platelet geometry of GnP shields CNT fillers from fracture and damage during processing, meanwhile still realizing the full dispersion of both nanofillers during high power sonication, thus resulting in greatly improved electrical conductivity, thermal conductivity and dynamic mechanical properties. Shin *et al*. achieved ultra-tough poly(vinyl alcohol) fibers containing CNT-reduced graphene oxide flake mixture. They found that the super-tough property is attributed to the formation of an interconnected network of partially aligned nanofillers during solution spinning[25]. Mechanically robust, magnetic nylon-6 nanocomposites reinforced by 1D CNT and 2D clay nanoplatelet hybrids also have been obtained using a simple melt-compounding technique in our previous study[26]. The direct iron-catalyzed chemical vapor deposition growth of CNTs utilizes iron oxide-immobilized clay nanoplatelets as substrates, carrying out *in situ* intercalation and exfoliation of clay nanoplatelets. Thus, the as-obtained heterostructured hybrids are demonstrated to be ideal and excellent nanofillers for fabricating nylon-6 nanocomposites with high performance and multi functionality.

Our previous study indicates that, with the addition of only 1 wt% organo-modified CoAl-LDHs into the neat PA6, although its mechanical property is substantially improved, but the tensile modulus seems difficult to be further improved with increasing CoAl-LDH content[27]. Therefore, we describe a synergistic approach to improve the mechanical properties of PA6 matrix by simultaneously using both CNTs and CoAl-LDHs with unique geometry and aspect ratio in this work. The synergistic effect of LDH and CNT nanofillers on the mechanical properties of ternary PA6/LDH/CNT composites has also been investigated.

EXPERIMENTAL

Materials

ε-Caprolactam and 6-aminocaproic acid (chemical reagent grade) were purchased from Shanghai Chemical Reagents Company and used without further purification. Multi-walled CNTs were prepared by catalytic chemical vapor deposition of methane on Co-Mo/MgO catalysts[28], and purified by dissolving the catalyst in hydrochloric acid followed by refluxing in nitric acid to increase more carboxylic and hydroxyl groups, as described in detail elsewhere[29]. Organo-modified CoAl-LDH (OCoAl-LDH) was prepared according to the literature[27].

Preparation of Binary PA6/LDH and PA6/CNT Composites and Ternary PA6/LDH/CNT Composites

A desired amount of OCoAl-LDHs, CNTs and 40 g of ε-caprolactam were placed into a three-necked round bottom flask. The mixture was sonicated at 80 °C for 90 min, and then 4 g of 6-aminocaproic acid were added to

the suspension. The flask was transferred to a preheated oil bath (250 °C) and heated for 6 h with mechanical stirring under a nitrogen atmosphere. The products were mechanically crushed and soaked in boiling water for 1 h to extract the unreacted monomers and oligomers, followed by drying at 90 °C under vacuum for 24 h for subsequent characterization.

Characterization

Film samples (with a thickness of 0.5 mm) were prepared by compression molding with a hot press at 250 °C, followed by quenching in an ice/water bath. The obtained films were finally punched into dog-bone specimens with a dimension of 63.5 mm × 9.53 mm × 0.50 mm (ASTM D-638 Type V) using a CEAST hollow die punch (model 6051). The tensile tests were carried out using an Instron universal material testing system (Model 5567) at room temperature with a gauge length of 25 mm and crosshead speed of 5 mm/min. At least six specimens were tested for neat PA6 and its nanocomposites.

X-ray diffraction (XRD) experiments were conducted on a Bruker diffractometer using CuKα radiation. The crystallinities (X_c) of the samples were estimated by XRD. A scanning electron microscope (SEM) (JEOL JSM 6700F) was used to observe the morphology of the failure surfaces of PA6 composites. Transmission electron microscope (TEM) images were recorded on a Philips CM300 FEG TEM operated at 200 kV. Thin sections (with a thickness of about 80 nm) for TEM observations were cut under cryogenic conditions using a Leica microtome with a diamond knife.

Nanoindentation tests were performed by an MTS Nano Indenter with a continuous stiffness measurement (CSM) technique. A three-sided pyramid (Berkovich) diamond indenter was employed. PA6 and composite films were mounted on flat aluminum stubs by superglue. During the tests, indenter was pressed into the materials with a constant strain rate, *i.e.*, 0.05 s^{-1}, from the surface to 5000 nm deep into the surface. Here, a constant strain rate was chosen to load on the samples in order to avoid a strain-hardening effect. At least 10 indentations were performed on each sample, and the interval between each two indentations was 100 μm apart in order to avoid interaction.

Rheological properties of neat PA6 and its composites were measured on a strain-controlled rheometer (ARES, TA Instruments). Small-amplitude oscillatory shear measurements were performed to obtain resultant shear stress using parallel-plate geometry with a plate diameter of 25 mm and a plate gap setting of 1.0 mm. To maintain all the rheological experiments in the linear viscoelastic region, strain sweeps were performed in advance for each sample, and consequently a strain of 1% was selected for all frequency sweep data. The rheological properties were reproducible after repeated temperature cycling and frequency sweep, indicating that there was almost no chain degradation during rheological measurements.

RESULTS AND DISCUSSION

Figure 1 shows the XRD patterns of OCoAl-LDH, neat PA6, PA6/LDH, PA6/CNT and PA6/CNT/LDH composites with different filler contents. The basal spacing (d_{003}) of OCoAl-LDH has been calculated to be 2.53 nm (2θ = 3.46°), which is in good agreement with that reported previously[30]. After polymerization, the characteristic (003) reflection of OCoAl-LDH disappears for both PA6/LDH and PA6/CNT/LDH composites. This indicates a collapse of the lamellar structure of LDH stacks, thus forming a disordered or exfoliated nanostructure within the matrix. It also indicates that the presence of CNTs does not affect the exfoliation of LDHs in PA6. Furthermore, two main diffraction peaks are observed at 2θ = 20° and 23.7° in the XRD patterns, which are assigned to α(200) and α(002/202) crystal planes of PA6 respectively. After the incorporation of CNTs or/and LDHs into the matrix, no significant change in the crystalline phase of PA6 is observed. The crystalline peaks only become slightly stronger and sharper, implying an enhanced crystallinity. It is reported that the α-phase crystals of PA6 exhibit a higher modulus than the less stable γ-phase[31]. Therefore, the α-form population is the dominant crystalline phase in all PA6 nanocomposites prepared here, which may in fact contributes to the mechanical property enhancement.

TEM can give direct evidence on the filler dispersion state in the composites, allowing a good assessment of the dispersion morphology of the nanofillers. Figure 2 shows the TEM images of the ultrathin sections of ternary PA6/1 wt% LDH/0.5 wt% CNT, PA6/1 wt% LDH/2 wt% CNT composites and their parental binary composites obtained by *in situ* polymerization. It can be clearly seen that the CNTs are evenly distributed in the polymer matrix (Figs. 2a and 2c), even at high concentration of 2 wt% in PA6/CNT composites (Fig. 2c). Due to their small size, high aspect ratio and large surface area, CNTs often exist in bundle or self-agglomerate at high concentrations. Thus, a few entanglements or bundles of CNTs are occasionally observed in PA6 composite with 2 wt% CNTs (Fig. 2c). The typical exfoliated morphology of PA6 nanocomposite with 1 wt% LDHs is shown in Fig. 2(e). The dark regions represent the LDH layers, whereas the bright areas represent PA6 matrix. It is evident that the stacked LDH layers lose their ordered-layer structures and are randomly distributed in the PA6 matrix, which is consistent with the XRD results presented in Fig. 1.

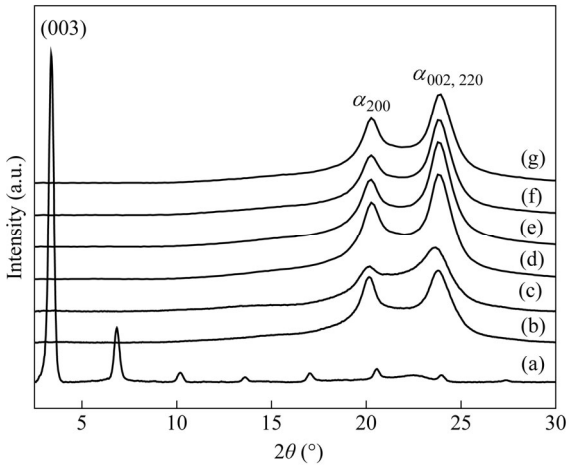

Fig. 1 XRD patterns of OCoAl-LDH, neat nylon-6 and its nanocomposites with different filler contents: (a) OCoAl-LDH, (b) neat PA6, (c) PA6/1 wt% LDH, (d) PA6/0.5 wt% CNT, (e) PA6/2 wt% CNT, (f) PA6/0.5 wt% CNT/1 wt% LDH and (g) PA6/2 wt% CNT/1 wt% LDH

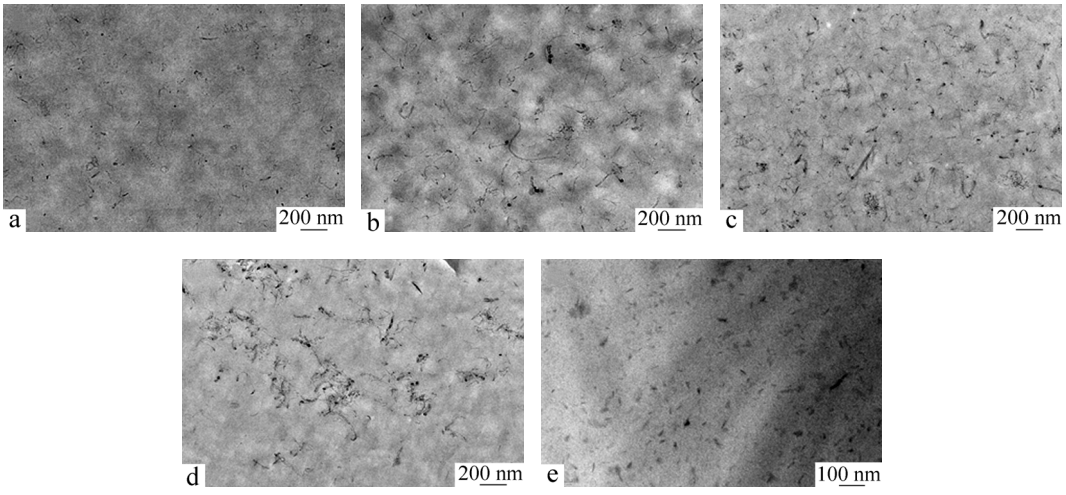

Fig. 2 TEM images of PA6 nanocomposites with different filler contents: (a) PA6/0.5 wt% CNT, (b) PA6/0.5 wt% CNT/1 wt% LDH, (c) PA6/2 wt% CNT, (d) PA6/2 wt% CNT/1 wt% LDH and (e) PA6/1 wt% LDH

With the incorporation of both LDHs (1 wt%) and CNTs (0.5 wt%) into PA6 matrix, the TEM image (Fig. 2b) shows that the CNTs are well-dispersed with no aggregates observed. Meanwhile, it is very interesting

to observe that some CNTs are located within the LDH platelet regions, where the CNTs are connected with the LDH platelets thus forming LDH-CNT network. In this unique filler network, the motion of CNTs in PA6 matrix is probably restrained by LDH platelets during deformation, which may result in an enhanced interaction between PA6 chains and the fillers. Based on the XRD results and TEM observations, it can be concluded that the ternary PA6/CNT/LDH nanocomposites with an exfoliated structure of LDHs and well-dispersed CNTs have been successfully prepared through *in situ* polymerization.

For the nanocomposites containing 2 wt% CNTs, however, the addition of 1 wt% LDH platelets leads to entangled or clustered CNTs, resulting in severe aggregation of nanotubes (Fig. 2d). Close inspection on the binary PA6 nanocomposites containing 2 wt% CNTs (Fig. 2c) or 1 wt% LDHs (Fig. 2e) shows that both CNTs and LDHs are homogeneously distributed in PA6 matrix. For the ternary PA6/CNT-LDH composite, we can see that the LDH aggregates are surrounded by a sea of CNTs and the nanotubes are not observed in the open areas that have little or no LDH platelets; this suggests that a strong affinity exists between the two kinds of nanofillers, as schematically illustrated in Fig. 3. This affinity is probably originated from the electrostatic and hydrogen bonding interactions between the carboxylated CNTs and the positively charged LDHs with abundance of hydroxyl groups. Clearly, the formation of such unique CNT-LDH hybrid network not only greatly prevents the aggregation among CNTs but also effectively prohibits the stacking or clustering among LDH platelets, which is favorable for their fine dispersion throughout the matrix. Therefore, a synergistic dispersion or co-exfoliation for both CNTs and LDHs can be realized by forming such unique CNT-LDH hybrid network.

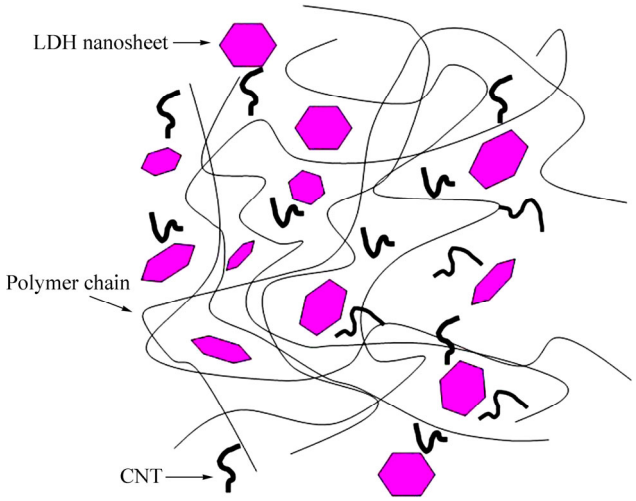

Fig. 3 Schematic illustration of physical jamming of 2D LDH nanoplatelets with 1D CNTs, forming a 3D percolated network

The mechanical properties and crystallinity of the binary and ternary PA6 composites are summarized in Table 1. Nanoindentation is a simple but powerful technique, which can provide useful information about the mechanical properties (such as elastic modulus and hardness) of materials in an easy and quick way. Due to its localized nature, the indentation test shows its advantages than the conventional tensile test by providing information on heterogeneity of material[27]. Figures 4(a) and 4(b) show the hardness and modulus profiles with respect to displacement into the sample surfaces for neat PA6 and its composites. The results of hardness and modulus are the averaged values in the depth between 4000 nm and 5000 nm. When indentation depth approaches beyond 2000 nm, the profiles show stable trends for all the samples, indicating that the CNTs or LDHs are homogeneously dispersed along the indention direction.

The remarkable synergistic effect of both CNTs and LDHs on the reinforcement of PA6 is clearly demonstrated in Fig. 4. With the incorporation of both LDHs (1 wt%) and CNTs (0.5 wt%), the hardness of the ternary nanocomposites is significantly increased by 110% from 0.063 GPa to 0.132 GPa and elastic modulus is

greatly increased by 150% from 1.13 GPa to 2.82 GPa, compared to neat PA6. Both the hardness and elastic modulus of ternary PA6/CNT-LDH composite are much higher than those of the corresponding binary PA6/1 wt% LDH and PA6/0.5 wt% CNT composites (Table 1). It is worthwhile to mention that even when 2 wt% CNTs alone are incorporated into PA6 matrix, the optimum hardness and elastic modulus of the binary composite are 0.111 GPa and 2.36 GPa respectively, which is obviously inferior than the ternary one with only 0.5 wt% CNTs and 1 wt% LDHs. Furthermore, the LDHs are either available as naturally occurring or can be conveniently synthesized on a large scale in an economical way[8]; while high cost and limited availability are the main obstacles for wide applications of the CNTs. Thus, the advantages and uniqueness of using CNT-LDH synergy to make high-performance polymer nanocomposites are obvious. In addition, it is worthwhile to note that the modulus data, as shown in Table 1, by the two techniques (*i.e*. nanoindentation and tensile tests) have similar changing trends but with different absolute values. The possible origins for the discrepancy may be due to the different loading directions and the frequency used for the two measurements[18]. From the tensile tests, the yield strength and tensile modulus of the ternary PA6/CNT-LDH composite are respectively confirmed to be 69.3 MPa and 3.3 GPa, which are much higher than the yield strength (50 MPa) and tensile modulus (1.7 GPa) of those of nylon-6/(CNT-clay) composite reported previously[26], which indicates the superiority of the combination of 1D CNTs and 2D LDHs in property enhancement of polymer composites.

Table 1. Summary of the mechanical properties of neat PA6 and its nanocomposites as a function of CNT and LDH concentrations

Samples	Hardness (GPa)	Modulus by nanoindentation (GPa)	Modulus by tensile tests (GPa)	Yield strength (MPa)	Elongation at break (%)	Crystallinity (%)
Neat PA6	0.063 ± 0.004	1.13 ± 0.05	1.0 ± 0.1	30.5 ± 0.7	195.2 ± 8.5	33%
PA6/1 wt% LDH	0.079 ± 0.055	1.49 ± 0.08	2.0 ± 0.1	53.1 ± 1.9	86.9 ± 9.5	39%
PA6/0.5 wt% CNT	0.096 ± 0.005	1.89 ± 0.05	2.8 ± 0.2	60.1 ± 1.6	95.4 ± 4.2	37%
PA6/0.5 wt% CNT/ 1 wt% LDH	0.132 ± 0.011	2.82 ± 0.11	3.3 ± 0.2	69.3 ± 0.8	34.9 ± 2.3	38%
PA6/2 wt% CNT	0.111 ± 0.007	2.36 ± 0.08	3.2 ± 0.1	64.8 ± 3.2	45.3 ± 4.8	41%
PA6/2 wt% CNT/ 1 wt% LDH	0.106 ± 0.003	2.25 ± 0.09	2.8 ± 0.1	50.4 ± 1.0	10.5 ± 3.1	39%

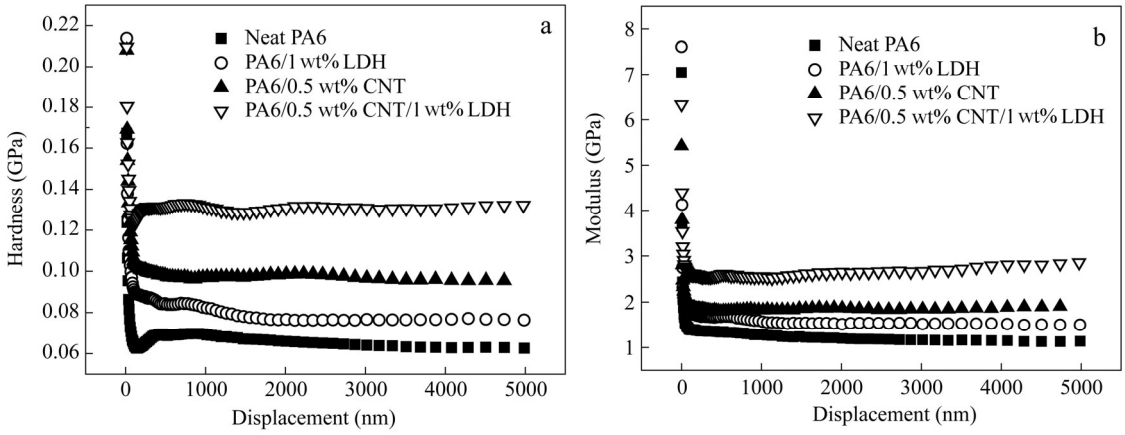

Fig. 4 Hardness (a) and modulus (b) profiles with respect to the displacement into sample surfaces for neat PA6 and its nanocomposites as a function of different filler contents

It has been reported that an increase in SWNT content in poly(vinyl alcohol) (PVA) composites leads to a linear increase in the crystallinity of PVA along with a crystalline coating of PVA on SWNTs[32]. This crystalline coating of PVA on SWNTs was proposed to be responsible for the improved mechanical properties of PVA composites. In comparison, the overall crystallinity of PA6 remains almost unchanged (37%–41%) in the ternary

or binary PA6 composites, as shown in the XRD patterns and Table 1. Obviously, the change in crystallinity plays less important role here in further improvement of the mechanical properties for ternary PA6/LDH-CNT composites, as compared with PA6/CNT composites. Hence, it can be assumed that the enhancement in tensile strength and modulus is not related to the changes in the degree of crystallinity and crystal structure of PA6.

Rheological measurement is a powerful tool to investigate the interactions in a composite system. In order to shed some light on the origins of the above mentioned synergistic effect, the melt rheological behavior of the composites was studied. The storage modulus (G') of the composites as a function of frequency (ω) at 230 °C is shown in Fig. 5. At low ω range, the rheological properties can be considered to reflect the relaxation and motion of the whole polymer chains. At high ω range (which corresponds to the chain movement within small time-scale), no significant difference in G' is seen for the composites with different nanofillers. At low ω range, the polymer chains are fully relaxed and exhibit homopolymer-like terminal behavior for PA6. With the incorporation of CNTs or LDHs into the matrix, the dependence of G' on ω becomes comparatively weak. It is interesting to note that, for the ternary PA6/LDH-CNT composite, the slope of the storage modulus curve is much less frequency dependent at low deformation frequencies. This non-terminal solid-like rheological behavior suggests the formation of an interconnected or network-like structure, thus the free movement of PA6 chains is restricted by the spatially confined geometry.

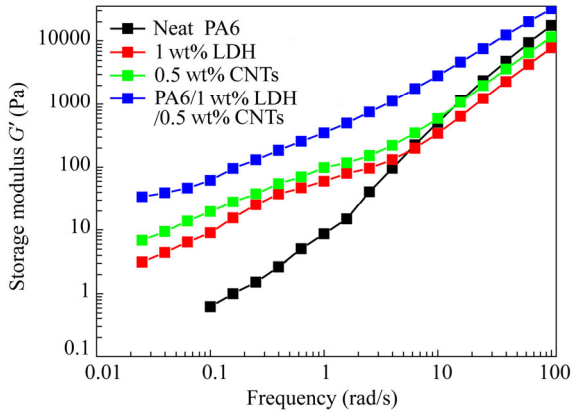

Fig. 5 Frequency response of storage modulus (G') for PA6 and its nanocomposites at 225 °C

By combining the rheological results with the TEM observations, we may conjecture that the synergistic effect between CNTs and LDHs in markedly improved mechanical properties of PA6 is crucially attributed to the formation of an interpenetrating network structure (as illustrated in Fig. 3) as well as the unique interactions between CNTs and LDHs. Indeed, on one hand, it is possible that the CNTs are intercalated between the layers of the LDHs, thereby weakening layer-to-layer interactions. This leads to enlarged or swollen layer distance which ultimately facilitates the delamination of LDHs and the intercalation of PA6 chains. As a result, the LDHs are easily exfoliated or delaminated into platelets throughout the matrix, which is beneficial for the overall improvement of the mechanical property. On the other hand, the aggregation of the CNTs can effectively be prohibited by the exfoliated LDH sheets due to their unique 2D spatial shielding effect. Thus, this CNT-LDH interlocked structure is endowed with better mechanical properties of ternary PA6 composites as compared with those of neat PA6 and its binary composites.

In fact, the rheological data have indicated the formation of the superposition of different networks, which probably result from different interactions in the composites. For example, apart from —OH and —COOH groups on the surface of CNTs due to the acid treatment, there exists polar interaction between the hydroxyl groups of LDH layers and —CONH— groups of PA6 chains *via* hydrogen bonding, thus forming a conjugated hydrogen bonding network. These multiple interfacial interactions may inhibit phase separation and are favorable for the enhancement of mechanical properties during deformation.

More interestingly, the CNT content has a distinct effect on the synergistic reinforcement of LDHs and CNTs for PA6 matrix. When CNTs alone are added, the Young's modulus and the yield strength of the composites are improved steadily as the CNT loading increases from 0.5 wt% to 2 wt%, indicating that higher loading may provide more property enhancement. However, the presence of LDHs, even though with the addition of only 1 wt%, in the ternary composites significantly alters this trend. The mechanical properties are found to be dramatically decreased with the increase of filler loading. For example, the yield strength of PA6/1 wt% LDH/2 wt% CNT composite (50.4 MPa) turns out to be less than expected, which is markedly inferior to that of PA6/1 wt% LDH/0.5 wt% CNT (69.3 MPa), and even lower than that of the corresponding binary PA6/ 2 wt% CNT composite (64.8 MPa).

Figures 6(a) and 6(b) show the SEM images of the cryogenically fractured surfaces of PA6/2 wt% CNT and PA6/2 wt% CNT/1 wt% LDH samples respectively. It can be seen that for PA6/2 wt% CNT, the CNTs which appear as bright spots due to their high electrical conductivity are evenly dispersed throughout the matrix (Fig. 6a); this observation is also in agreement with TEM image (Fig. 2c). Moreover, the presence of the well-dispersed broken nanotubes and the absence of nanotube aggregation on the fracture surface of the composite indicate strong interfacial interaction between PA6 and the nanotubes. This is probably due to the chemical modification during purification with nitric acid treatment, thus increases the polarity of the nanotubes and improves the compatibility as well as interfacial adhesion between the nanotubes and PA6 matrix. The good dispersion of the CNTs in the matrix provides more uniform stress distribution and minimizes the presence of stress-concentration centers, thus increasing the interfacial area and facilitating the stress transfer from the polymer matrix to the nanotubes. As a result, the mechanical properties of the PA6/CNT composites are significantly improved with the addition of CNTs into PA6 matrix. In sharp contrast, the fractured surface of PA6/2 wt% CNT/1 wt% LDH composite shows some areas are without CNTs and some other areas with CNT aggregations, as indicated by white arrows (Fig. 6b). Similar morphology is also observed in the ultrathin section of PA6/2 wt% CNT/1 wt% LDH composite by TEM (Fig. 2d). The non-uniform dispersion of CNTs in the matrix may induce stress concentration sites and makes the composite easy to fail, thus limiting its potential strengthening effect. At a given loading level of LDHs (*i.e.*, 1 wt%), when the CNT content increases from 0.5 wt% to 2 wt%, some agglomerations are likely to occur due to inter-tube van der Waals attractions. However, the strong interactions between LDHs and CNTs may lead to the re-aggregation or re-stacking of the exfoliated LDH nanoplatelets, even for the case of slight CNT aggregation. This results in secondary aggregations and entanglements of the dispersed CNTs, which leads to even more simultaneous aggregation of CNTs and LDHs. This templated dispersion of CNTs and LDHs in PA6/1 wt% LDH/2 wt% CNT composite is schematically shown in Fig. 7. Therefore, it is not surprising that the mechanical properties of the ternary PA6/CNT/LDH composites deteriorate as the CNT loading increases, which is due to poor dispersion of nanofillers in the matrix, as shown in Table 1. Therefore, the difference in the morphologies of the cryo-fractured surface of PA6/2 wt% CNT and PA6/2 wt% CNT/1 wt% LDH composites is in fact a good indication for the unique interactions between the CNT and LDH nanofillers.

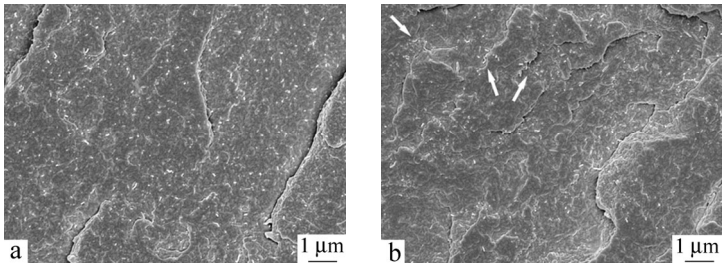

Fig. 6 SEM images showing an overall morphology of failure surface for (a) binary PA6/2 wt% CNT nanocomposite and (b) ternary PA6/2 wt% CNT/1 wt% LDH nanocomposite

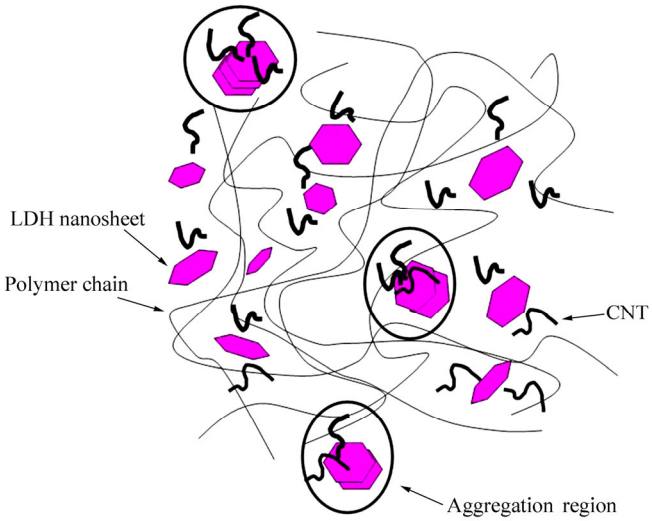

Fig. 7 Schematic illustration of network formation within PA6/2 wt% CNT/1 wt% LDH nanocomposite

CONCLUSIONS

PA6 nanocomposites with various inorganic contents have been prepared by *in situ* polymerization. The synergistic effect of 2D LDH platelets and 1D CNTs in improving the mechanical properties of PA6 has been examined and discussed. TEM observations show the formation of LDH-CNT hybrid network, where the LDH platelets are likely to impede the motion of CNTs in PA6 matrix during deformation as well as enhancing the interaction between PA6 chains and the fillers. On the other hand, the LDH nanoparticles are also found to promote much greater aggregation at high CNT content (2 wt%), indicating strong interaction between the LDHs and CNTs. This results in significant deterioration in the mechanical properties of the obtained composite. Therefore, the optimization of both the concentration of CNTs or LDHs and their unique interactions plays an important role in the property enhancement of PA6 composites. This work shows that the combination of 1D CNTs and 2D LDHs exhibits intriguing potential in obtaining high-performance PA6 nanocomposites, thus extending the practical applications of PA6.

REFERENCES

1 Paul, D.R. and Robeson, L.M., Polymer, 2008, 49(15): 3187
2 Usuki, A., Kojima, M., Okada, A., Fukushima, Y., Kurauchi, T. and Kamigatio, O., J. Mater. Res., 1993, 8(5): 1179
3 Pavlidou, S. and Papaspyides, C.D., Prog. Polym. Sci., 2008, 33(12): 1119
4 Liu, T.X., Chen, D., Phang, I.Y. and Wei, C., Chinese J. Polym. Sci., 2014, 32(1): 115
5 Rajini, N., Winowlin Jappes, J.T., Rajakarunakaran, S. and Bennet, C., Chinese J. Polym. Sci., 2013, 31(8): 1074
6 Nshuti, C.M., Wang, D.Y., Hoessenlopp, J.M. and Wilkie, C.A., J. Mater. Chem., 2008, 18(26): 3091
7 Pradhan, S., Costa, F.R., Wagenknecht, U., Jehnichen, D., Bhowmich, A.K. and Heinrich, G., Eur. Polym. J., 2008, 44(10): 3122
8 Leroux, F. and Besse, J.P., Chem. Mater., 2001, 13(10): 3507
9 Yu, W.W., Fu, H.K., Zhang, D.Z., Du, M. and Zheng, Q., Acta Polymerica Sinica (in Chinese), 2013, (09): 101
10 Costache, M.C., Heidecker, M.J., Manias, E., Camino, G., Frache, A., Beyer, G., Gupta, R.K. and Wilkie, C.A., Polymer, 2007, 48(22): 6532
11 Coleman, J.N., Khan, U. and Gun'ko, Y.K., Adv. Mater., 2006, 18(6): 689
12 Henley, S.J., Hatton, R.A., Chen, G.Y., Gao, C., Zeng, H.L., Kroto, H.W. and Silva, S.R.P., Small, 2007, 3(11): 1927
13 Gao, Y., Zong G.Y., Bai, H.W. and Fu, Q., Chinese J. Polym. Sci., 2014, 32(2): 245

14 Huang, Z.Z., Song, Y.H., Tan, Y.Q. and Zheng, Q., Acta Polymerica Sinica (in Chinese), 2013,(1): 88
15 Gao, J.B., Itkis, M.E., Yu, A., Bekyarova, E., Zhao, B. and Haddon, R.C., J. Am. Chem. Soc., 2005, 127(11): 3847
16 Gao, J.B., Zhao, B., Itkis, M.E., Bekyarova, E., Hu, H., Kranak, V., Yu, A.P. and Haddon, R.C., J. Am. Chem. Soc., 2006, 128(23): 7492
17 Zhang, W.D., Shen, L., Phang, I.Y. and Liu, T.X., Macromolecules, 2004, 37(2): 256
18 Liu, T.X., Phang, I.Y., Shen, L., Chow, S.Y. and Zhang, W.D., Macromolecules, 2004, 37(12): 7214
19 Meng, H., Sui, G.X., Fang, P.F. and Yang, R., Polymer, 2008, 49(2): 610
20 Chen, G.X., Kim, H.S., Park, B.H. and Yoon, J.S., Polymer, 2006, 47(13): 4760
21 Tang, C.Y., Xiang, L.X., Su, J.X., Wang, K., Yang, C.Y., Zhang, Q. and Fu, Q., J. Phys. Chem. B, 2008, 112(13): 3876
22 Sumfleth, J., Adroher, X. and Schulte, K., J. Mater. Sci., 2009, 44(12): 3241
23 Prasad, K.E., Das, B., Maitra, U., Ramamurty, U. and Rao, C., Proc. Natl. Acad. Sci., 2009, 106(32): 13186
24 Kumar, S., Sun, L., Caceres, S., Li, B., Wood, W., Perugini, A., Maguire, R.G. and Zhong, W.H., Nanotechnology, 2010, 21: 105702
25 Shin, M.K., Lee, B., Kim, S.H., Lee, J.A., Spinks, G.M., Gambhir, S., Wallace, G. G., Kozlov M.E., Baughman R.H. and Kim, S.J., Nat. Commun., 2012, 3: 650
26 Zhang, C., Tjiu, W.W., Liu, T.X., Lui, W.Y., Phang, I.Y. and Zhang, W.D., J. Phys. Chem. B, 2011, 115(13): 3392
27 Peng, H.D., Tjiu, W.C., Shen, L., Huang, S., He, C.B. and Liu, T.X., Compos. Sci. Technol., 2009, 69(7–8): 991
28 Bacsa, R.R., Laurent, C., Peignery, A., Bacsa, W.S., Vaugien, T. and Rousset, A., Chem. Phys. Lett., 2000, 323(5): 566
29 Goh, H.W., Goh, S.H., Xu, G.Q., Pramoda, K.P. and Zhang, W.D., Chem. Phys. Lett., 2003, 379(3–4): 236
30 Liu, Z.P., Ma, R.Z., Osada, M., Iyi, N., Ebina, Y., Takada, K. and Sasaki, T., J. Am. Chem. Soc., 2006, 128(14): 4872
31 Lincoln, D.M., Vaia, R.A., Wang, Z.G. and Hsiao, B.S., Polymer, 2001, 42(4): 1621
32 Cadek, M., Coleman, J.N., Ryan, K.P., Nicolosi, V., Bister, G., Fonseca, A., Nagy, J.B., Szostak, K., Béguin, F. and Blau, W.J., Nano Lett., 2004, 4(2): 353